Research and Development Technical Report
CECOM-TR-94-D617-F

COMMON CONTROL MODULE FOR PHOTONICALLY CONTROLLED PHASED ARRAYS

Dr. Walter Charczenko
Dr. Michael J. LaGasse
Dr. Suwat Thaniyavarn

Boeing Defense & Space Group
P.O. Box 3999, MS 3W-51
Seattle, Washington 98124

August 1996

CECOM
U.S. ARMY COMMUNICATIONS-ELECTRONICS COMMAND
RESEARCH, DEVELOPMENT AND ENGINEERING CENTER
FORT MONMOUTH, NEW JERSEY 07703-5203

NOTICES

Disclaimers

The findings in this report are not to be construed as an official Department of the Army position, unless so designated by other authorized documents.

The citation of trade names and names of manufacturers in this report is not to be construed as official Government endorsement or approval of commercial products or services referenced herein.

REPORT DOCUMENTATION PAGE

Form Approved
OMB NO. 0704-0188

1. AGENCY USE ONLY *(Leave blank)*	2. REPORT DATE	3. REPORT TYPE AND DATES COVERED
	August 1996	Final Report: Sep 94 to Mar 96

4. TITLE AND SUBTITLE
COMMON CONTROL MODULE FOR PHOTONICALLY CONTROLLED PHASED ARRAYS

5. FUNDING NUMBERS
C: DAAB07-94-C-D617
PE: 62782

6. AUTHOR(S)
Dr. Walter Charczenko, Dr. Michael J. LaGasse and Dr. Suwat Thaniyavarn

7. PERFORMING ORGANIZATION NAMES(S) AND ADDRESS(ES)
Boeing Defense and Space Group
P.O. Box 3999, MS 3W-51
Seattle, WA 98124

8. PERFORMING ORGANIZATION REPORT NUMBER

9. SPONSORING / MONITORING AGENCY NAME(S) AND ADDRESS(ES)
US Army Communications-Electronics Command (CECOM)
Space and Terrestrial Communications Directorate
ATTN: AMSEL-RD-ST-SY-TE (J. Wright)
Fort Monmouth, NJ 07703-5203

10. SPONSORING / MONITORING AGENCY REPORT NUMBER
CECOM-TR-94-D617-F

11. SUPPLEMENTARY NOTES
Space and Terrestrial Communications Directorate Project Engineer: James G. Wright, (908) 427-2819.

12a. DISTRIBUTION / AVAILABILITY STATEMENT
Approved for public release; distribution is unlimited.

12 b. DISTRIBUTION CODE

13. ABSTRACT *(Maximum 200 words)*

Photonic control of phased array antennas will allow fiber optic remoting of many antenna functions away from the front end of the antenna array. Integrated photonics is used to consolidate these operations onto a compact and low cost common module. The common module is independent of the frequency of operation of the antenna array. This program consisted of the design, development and demonstration of a 16-channel Integrated Phase and Amplitude Controller (IPAC) for performing two-dimensional phase and amplitude beam forming and steering operations. The photonic IPAC module was demonstrated at both Radio Access Point (RAP) Radio (6 to 12 GHz) and Wireless Local Area Network (LAN) (54 to 58 GHz) frequencies. Two-dimensional beam steering of a phased array antenna was verified using a simplified two signal control applied to the photonic controller. Photonic amplitude control of the antenna elements was shown to suppress antenna sidelobe levels for beam forming operations.

14. SUBJECT TERMS
Photonics; phased array; optical modulators; lithium niobate; optically controlled beam-forming/beam-steering

15. NUMBER IF PAGES
38

16. PRICE CODE

17. SECURITY CLASSIFICATION OR REPORT	18. SECURITY CLASSIFICATION OF THIS PAGE	19. SECURITY CLASSIFICATION OF ABSTRACT	20. LIMITATION OF ABSTRACT
Unclassified	Unclassified	Unclassified	UL

TABLE OF CONTENTS

LIST OF FIGURES

TABLE OF ACRONYMS

ARL	Army Research Laboratory
BT&D	British Telecom and Dupont
CECOM	Communications-Electronics Command
DC	direct current
EHF	extremely high frequency
EMC	electromagnetic compatibility
EMI	electromagnetic interference
EO	electro-optic
IF	intermediate frequency
IOC	integrated optical circuit
IPAC	integrated phase and amplitude controller
LAN	local area network
LO	local oscillator
$LiNbO_3$	lithium niobate
Nd:YAG	neodymium doped yttrium aluminum garnet
PIRI	Photonic Integration Research, Inc.
PM	polarization maintaining
RAP	radio access point
RF	radio frequency
SOS	silica-on-silicon
TE	transverse electric
Ti: $LiNbO_3$	titanium indiffused lithium niobate
TM	transverse magnetic

1.0 SUMMARY

This document is a final report describing the work completed under contract (DAAB07-94-C-D617) awarded to Boeing by U.S. Army CECOM on 15 June 1994. The work accomplished was in accordance with the statement of work entitled "Common Control Module for Photonically Controlled Phased Arrays" dated 14 October 1993, and is believed to completely satisfy the stated objectives of that statement of work. The objective of the contract was to design, develop, and test a two dimensional 16 channel photonic module for controlling an RF phased array antenna. The module was designed and demonstrated to work at both the (54 to 58 GHz) Wireless Local Area Network (LAN) and (6 to 12 GHz) Radio Access Point (RAP) frequency bands that are proposed in CECOM's Space and Terrestrial Communications Directorate "Communications-on-the-Move" program.

Photonics offers multiple advantages when applied to phased array antennas. Fiber optic corporate feed networks have several key advantages when compared to RF coaxial and waveguide systems. These advantages are:

- light weight,
- small cross section,
- low transmission loss,
- low signal dispersion,
- broad bandwidth,
- resistance to electromagnetic effects (EMI and EMC),
- common photonic modules for multiple RF bands, and
- increased signal processing capabilities.

The use of fiber optic feedlines also opens up the possibility of using photonic components to perform the beam forming and steering operations that have traditionally been done in the front end of phased array antennas. This will reduce the size and number of RF components at the front end of the phased array antenna while allowing the beam forming operations to be performed remotely in a compact module. This module can then be located in a secure location or electronics bay as far away as necessary from the antenna array front end.

The main objective of this program was to develop a fiber optic compatible photonic module for performing phased array antenna beam forming operations such as RF phase shifting and amplitude control for antenna beam steering. The key features of this module that were demonstrated during this program are:

- RF phase shifting for each antenna element,
- RF amplitude control for each antenna element,
- two dimensional beam steering with simplified control,
- optical control of antenna sidelobe levels, and
- compact common module operation independent of center RF frequency.

2.0 INTRODUCTION

2.1 BACKGROUND

Electronically controlled phased array antennas offer many advantages and features not available to single element antennas. The antenna beam steering capabilities of phased array antennas are necessary in many mobile communications scenarios such as CECOM's "Communications-on-the-Move" program. Currently, one disadvantage of phased array antennas is the requirement of individual electronic phase shifters at the front end of the antenna array. At higher frequencies this will limit either the spacing between the elements or the depth of a conformal antenna array. This will result in a degradation of the antenna performance with a narrower scanning angle.

The use of integrated photonic components for RF phase shifting can eliminate these problems. Using a fiber optic corporate feed network the integrated photonic phase shifters can be remoted away from the antenna array in a more secure environment. Integrated photonic phase shifters offer key advantages in phased array antennas in that they:

- eliminate dispersive electronic phase shifters,
- reduce area required for each antenna element,
- reduce the depth required for the conformal array,
- remote the phase shifting operation away from the antenna front end,
- incorporate new signal processing schemes with photonic phase shifting, and
- increase the bandwidth of the antenna.

Boeing is an established leader in the development of active phased arrays for EHF communications. In conjunction with this effort, Boeing has been aggressively developing photonic components and techniques for use in wideband analog systems such as phased array antennas. The use of polarization multiplexing techniques for RF antenna beam forming has been developed and patented here at the Microwave Photonics Laboratory (ref. 1,2). The implementation of this technique resulted in the design, development and delivery of a 16 channel Integrated Phase and Amplitude Controller (IPAC) for use in two dimensional phased array antennas. This common module was delivered to US Army CECOM at Ft. Monmouth, N.J.

2.2 PROGRAM OBJECTIVES AND TASKS

The main objective of this program was to develop a 16 channel common module photonic phase and amplitude controller for steering and beam forming a two dimensional phased array antenna independent of the center frequency. This program consisted of four major tasks:

- Task I: Design IPAC (including trade study),
- Task II: Develop Linear IPAC,
- Task III: Develop 2-dimensional IPAC, and
- Task IV: Integrate Beam Steering System.

Task I began with a definition of the RF beam forming operations required from the photonic processor. A trade study was completed to decide which photonic components were to be used in implementing the processing operations. In task II, a prototype 4 channel linear IPAC was developed and tested in a phased array testbed. Based on the results of these tests, a full two dimensional 16 channel IPAC was designed. This IPAC was developed during Task III of the program. Task IV consisted of demonstrating the operation of this IPAC in a phased array testbed. Antenna beam forming and steering demonstrations were performed over the U band for compatibility with the Wireless LAN frequencies (54 to 58 GHz) and at 7 GHz for compatibility with the RAP Radio frequencies (6 to 12 GHz). The same IPAC module was used at both sets of frequencies thereby demonstrating its invariance with the center frequency of operation.

2.3 PHASE AND AMPLITUDE CONTROL WITH INTEGRATED OPTICS

Integrated optical devices can be used to control the phase and amplitude of the microwave beat signals generated by an optical heterodyne signal. Figure 2.3-1 shows one such approach.

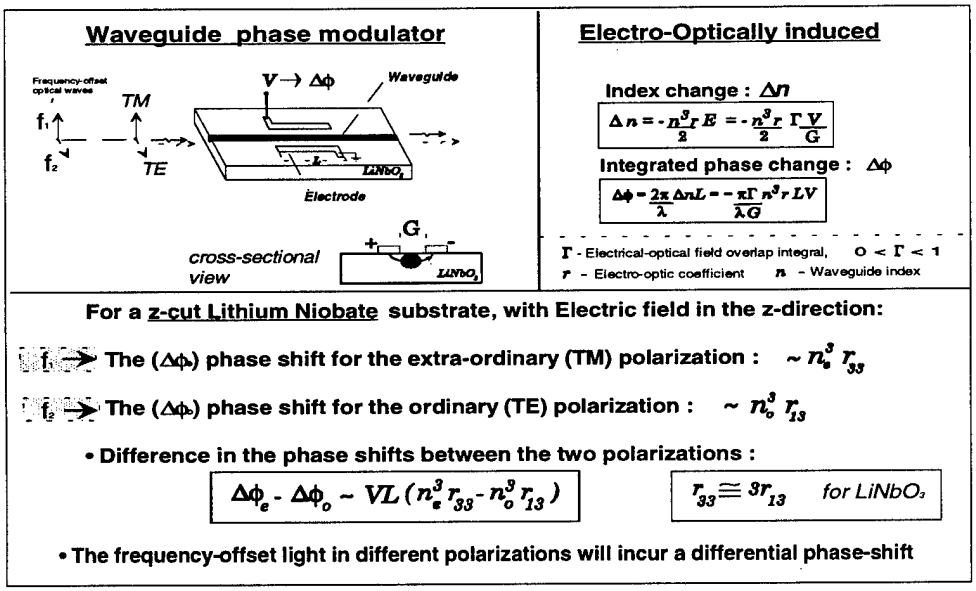

Figure 2.3-1. Phase Control with Orthogonal Polarizations

Two lasers are locked at frequencies f_1 and f_2. The two optical carriers are input to the integrated optical controller with orthogonal polarizations as shown in the figure. When a voltage is applied to the electrode on the device, an index change occurs in the crystal. The index change is different for the two polarizations. The index changes lead to a differential phase shift between the two optical carriers. In order to generate a heterodyne beat signal, a polarizer is placed between the integrated optical controller and the photodiode. The axis of polarizer must be rotated 45° relative to the integrated optical device axes for maximum efficiency. This orthogonal polarization approach has the advantage that the two carriers travel along the same path through the device. This minimizes common mode effects such as temperature gradients across the device.

It is also possible to control the amplitude of the microwave beat signal by using another integrated optical device such as a Mach-Zehnder modulator. The Mach-Zehnder can be integrated into the same substrate as the phase controller and adjusts the amplitude of both of the carriers. Finally, multiples of these integrated optical devices can be integrated into a common substrate to perform beam steering and forming operations for many elements of a phased array antenna.

2.4 REPORT OUTLINE

In this report we will present and discuss the results obtained over the course of this program. We begin with a presentation of the architecture and the results of the trade study for implementing this architecture. This will be followed by the results in developing a one dimensional 4 channel linear IPAC module. We will then present all of the issues in developing a two dimensional 16 channel IPAC. Test results in a phased array antenna testbed will be presented for U band (54 to 58 GHz) and RAP Radio frequencies (6 to 12 GHz) frequencies. Amplitude weighting of antenna elements for sidelobe suppression will also be presented.

3.0 COMMON CONTROL MODULE DEVELOPMENT

3.1 COMMON CONTROL MODULE ARCHITECTURE

A block diagram for the IPAC Common Control Module functions is shown in figure 3.1-1. The primary purpose of the module is to have each channel in the IPAC to provide RF phase and amplitude control to a corresponding antenna element of a phased array antenna via optical fiber. The IPAC consists of three submodules. These submodules are: the input optical splitter, the electro-optic (EO) controller, and a polarization combining section. A trade study was performed to determine the optimal components for each of these submodules. It was decided to use an integrated optic circuit (IOC) for splitting the optical power to the antenna elements as opposed to fiber optic splitters. The IOC 1xn splitters are more compact, lower in loss, and less susceptible to temperature and wavelength variations than their fiber counterparts. As the number of channels (n) increases, these advantages become more pronounced.

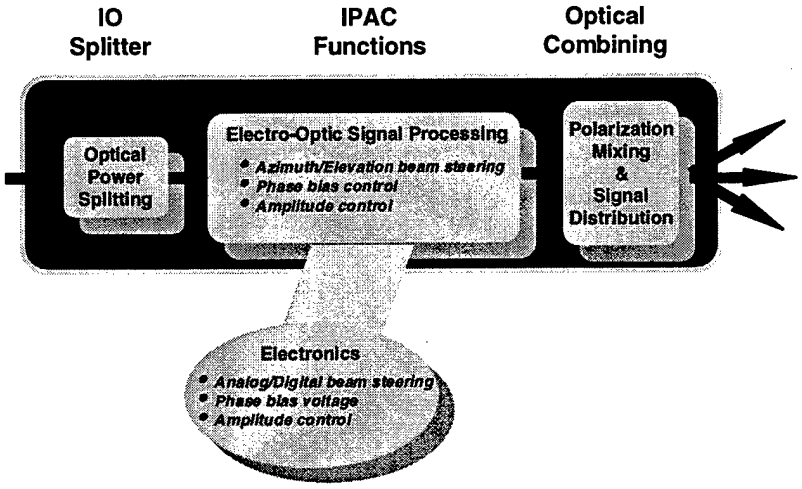

Figure 3.1-1. Block Diagram for IPAC Common Control Module Functions

The EO controller would consist of four sections on a common substrate. The first section would be used as a bias section to eliminate phase differences between orthogonal polarization states from channel to channel. The next two sections would use common mode electrodes to perform the antenna array beam steering in both the azimuth and elevation directions. A unique common mode electrode approach was used such that the beam steering could be performed in either direction with the application of a single applied voltage. The final section of the EO controller consisted of Mach-Zehnder interferometric devices for setting the amplitude of the optical signal to each of the RF antenna elements.

The output of the EO signal processing submodule consists of a polarizer section for combining the two (TE and TM) optical polarization states. Several possibilities were studied, including the use of on-chip polarizers, fiber optic inline polarizers with

polarization maintaining (PM) fiber and polarizing fiber. Polarizing fiber, utilizing silicon v-grooves for constructing fiber arrays, was the simplest and lowest cost of these technology alternatives.

3.2 1-DIMENSIONAL IPAC DEVELOPMENT AND CHARACTERIZATION

During task II, a 1-dimensional prototype IPAC was designed and fabricated to test the concepts. Integrated 1x4 optic splitters were fabricated both in-house in $LiNbO_3$ and purchased using Silica-on-Silicon (SOS) substrates from PIRI (Photonic Integration Research, Inc.). The EO submodule was designed on a $LiNbO_3$ substrate with titanium indiffused optical channels. The channels were designed to be low loss and single moded for both the quasi-TE and quasi-TM polarizations states. The electrodes consisted of a phase bias section, a linear beam steering section and a column of amplitude controllers. A four channel array of 3M polarizing fiber was used at the output. The polarizing fiber was rotated 45° with respect to the crystal axis of the EO controller and mounted in a silicon v-groove array by Wave Optics.

The submodules were butt-coupled to one another in a phased array testbed, such as the one shown in Figure 3.2-1. At the input, diode pumped Nd:YAG lasers were frequency offset to the U band (40 to 60 GHz). The orthogonal TE and TM optical polarization components were combined in a PM fiber and launched into a PIRI 1x4 integrated optic splitter. The PIRI/fiber assembly was mounted on a six axis translation stage and aligned to the $LiNbO_3$ EO controller. The polarizing fiber array was aligned to the output of the EO controller. The polarizing fiber combined the TE and TM modes from the IPAC and delivered the signal to four 60 GHz New Focus photodiodes. The photodiodes mixed the frequency offset lasers which generated a beat note in the U band (40 to 60 GHz) frequency range. The millimeter wave signals from the photodiodes were delivered to four horn antennas for transmission. A receiver consisted of a receiving horn antenna and an integrated LO quadrupler/low noise mixer/IF amplifier. The IF signal was detected using a spectrum analyzer. Several features of the Boeing IPAC were tested in this setup.

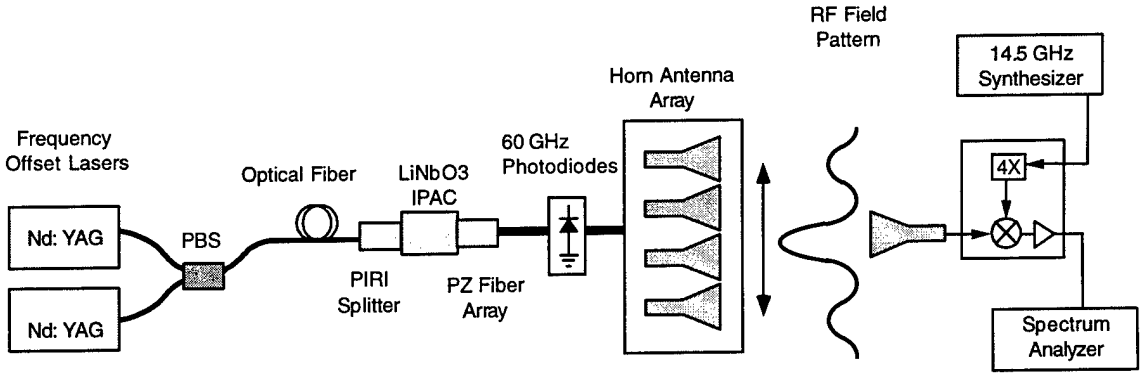

Figure 3.2-1. Optically Controlled Phased Array Testbed

One feature of the IPAC, is the ability to scan the direction of the main beam of a phased array antenna using a single applied voltage. Figure 3.2-2 shows a measured applied voltage ramp which steers the beam of the phased array antenna at broadside. The antenna array factor, AF, at broadside scales with this applied voltage as:

$$AF = \frac{1}{N}\left[\frac{\sin(\frac{N}{2}\beta)}{\sin(\frac{1}{2}\beta)}\right],$$

where N is the number of antenna elements (four) and β is the relative RF phase sweep between the antenna elements applied by the common phase shifter of the EO control section of the IPAC. In this manner, a single voltage sawtooth signal can sweep the antenna beam back and forth. Similarly, a single DC voltage applied to this electrode will point the main lobe of a phased array antenna in a fixed direction.

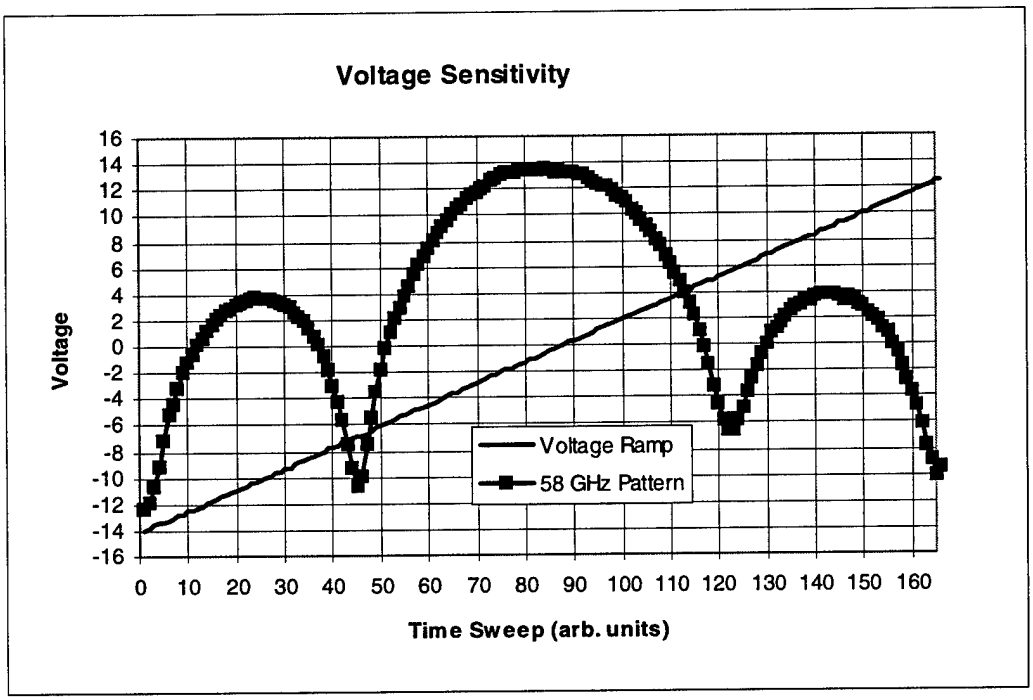

Figure 3.2-2. Broadside Antenna Pattern versus a Single Voltage Applied to the IPAC

A second important feature of the IPAC module that was demonstrated was the independence of the module to the center frequency of operation. The same IPAC module was tested over a variety of frequencies spanning the U band. Two such antenna patterns are shown below in Figure 3.2-3 for 44 GHz and 60 GHz respectively. The broadside signal was detected as a function of the common electrode voltage applied to the IPAC. The first nulls in the antenna pattern occur at ± 6 Volts. A good fit is obtained when comparing the measured data points to the calculated values taken from the array factor (*AF*).

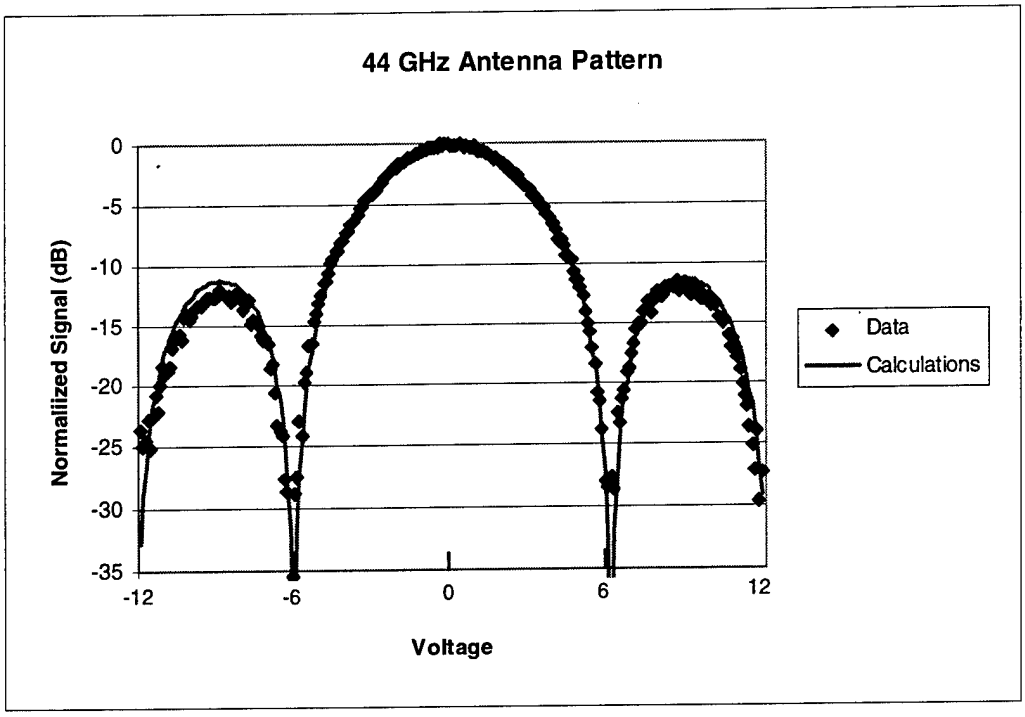

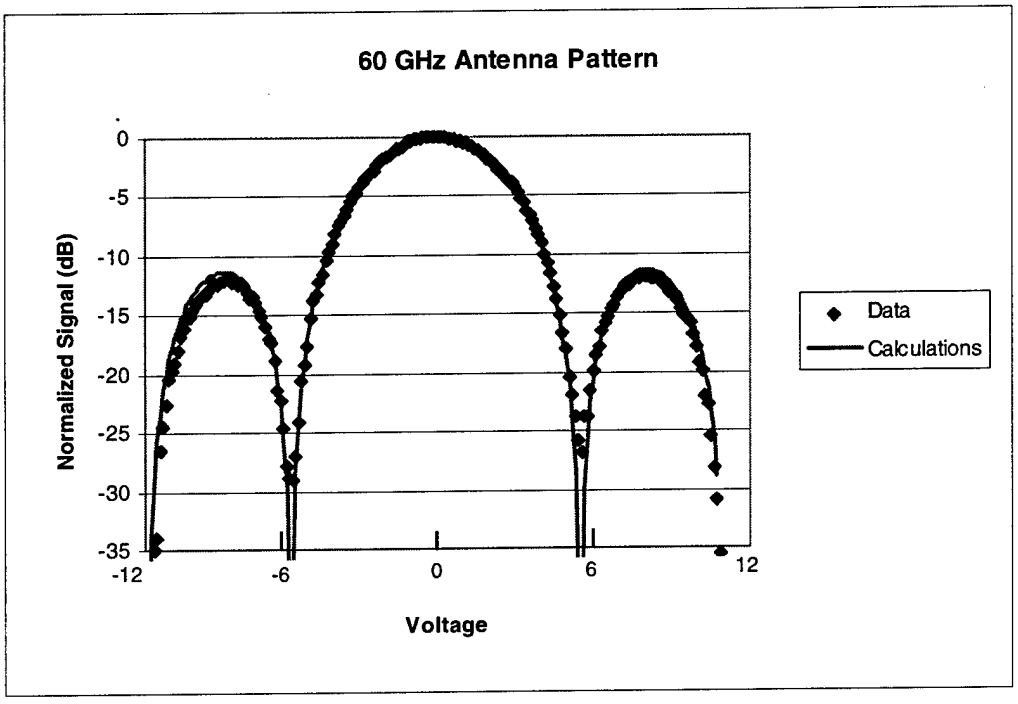

Figure 3.2-3. Measured 44 GHz and 60 GHz Optically Controlled Phased Array Patterns

3.3 DESIGN OF 16 CHANNEL TWO-DIMENSIONAL IPAC

Task III of this program consisted of designing, building, and testing a full two dimensional 16 channel IPAC. The design parameters for this IPAC were established based on measurements of the linear one dimensional 4 channel IPAC. The diagram of the 16 channel module is shown in Figure 3.3-1. The design criteria for each of these submodules (Power Splitter, EO Beam Controller, Polarization Combiner) are discussed in the following paragraphs.

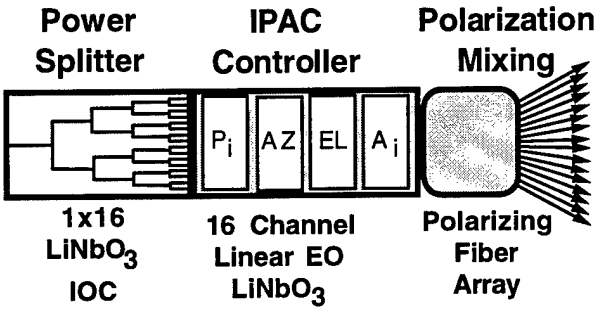

Figure 3.3-1. Two Dimensional 16 Channel Phased Array Controller Architecture

The IOC power splitter was implemented on a $LiNbO_3$ substrate. A comparison between a $LiNbO_3$ and a SOS 1x16 splitter is shown in Figure 3.3-2. The thermal coefficient differences and optical mode mismatch between the power splitter and the $LiNbO_3$ EO controller.are eliminated when using a $LiNbO_3$ substrate as opposed to the SOS process in manufacturing the IOC optical splitter.

	Silica on Silicon	Lithium Niobate
Chip Length (cm)	< 3	7
Optical Loss (dB)	< 2	< 2
$LiNbO_3$ Mode Mismatch (dB)	0.5 to 1.0	0
Fiber Mode Mismatch (dB)	0.1	0.4
Intrinsic Loss (dB/cm)	< 0.1	< 0.15
Thermal Mismatch (10^{-6} cm/cm/°C)	5 to 10	0
Polarization Crosstalk (dB)	15	30

Figure 3.3-2. Comparison between $LiNbO_3$ and SOS 1x16 IOC Optical Splitters

In addition, the SOS process results in waveguides with a polarization extinction ratio (ratio of TE to TM polarization) of only 10 to 15 dB. This was due to the low birefringence of the optical channels (which is necessary for telecommunications applications). As illustrated in Figure 3.3-3, the SOS optical waveguide birefringence is determined by the geometry of the waveguide. The $LiNbO_3$ waveguides exhibit a high birefringence due to the anisotropy ($\Delta n = n_o - n_e \sim 0.071$) of the crystal itself.

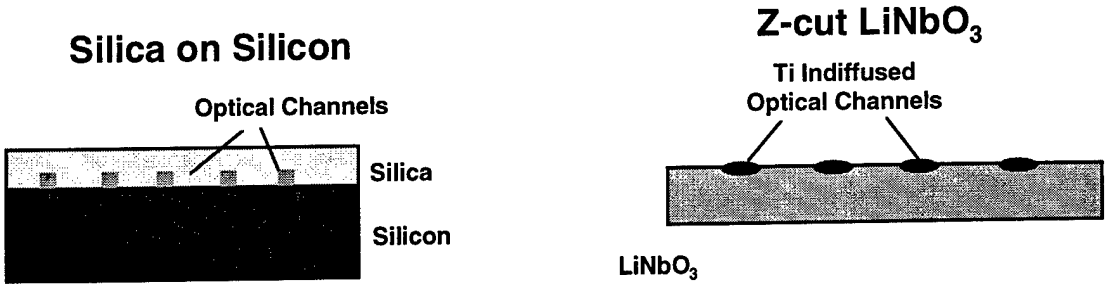

Figure 3.3-3. Cross Section View of SOS and $LiNbO_3$ Optical Waveguide Channels

A low polarization extinction ratio results in polarization crosstalk. Polarization crosstalk results in RF phase and amplitude errors at the individual antenna elements. A plot of this absolute amplitude error as a function of polarization crosstalk is given in Figure 3.3-4. In order to maintain an amplitude error of less than 5% the polarization extinction of the waveguides would have to be greater than 25 dB. This level of polarization crosstalk was not available from commercial SOS wafers. The disadvantage of $LiNbO_3$ splitters was that a more adiabatic Y-junction would have to be designed to maintain a low optical insertion loss level. This resulted in a longer device. One alternative approach for future optimization could be the use of a multi-mode interferometric splitter such as the one being investigated at the (ARL) Army Research Laboratory (ref. 3). In order to maintain the optical power budget, the 1x16 $LiNbO_3$ splitter would have to have a net insertion loss of less than 4 dB for both polarization states. This design criteria was met and exceeded, as is reported in the next section of this document.

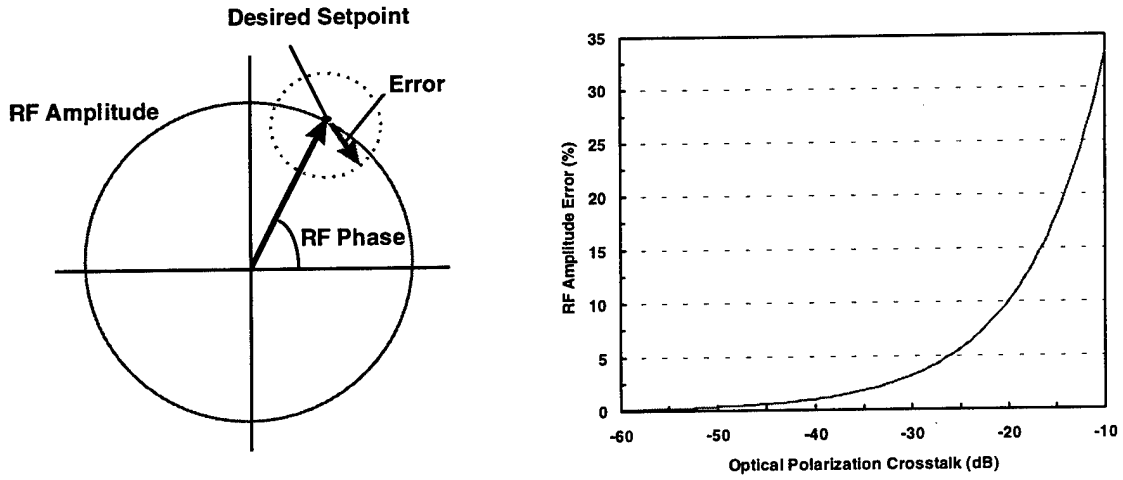

Figure 3.3-4. RF Antenna Amplitude Error from Optical Polarization Crosstalk

The EO controller was implemented using a Ti:$LiNbO_3$ waveguide technology. A schematic of a single channel is shown in Figure 3.3-5.

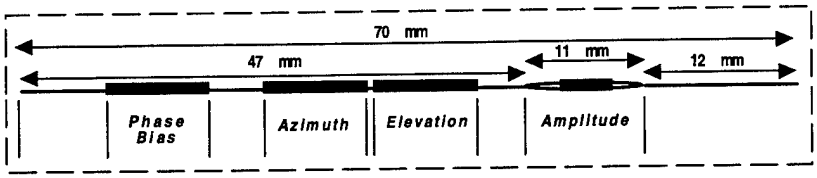

Figure 3.3-5. Schematic Layout and Dimensions for Single Channel of EO Controller

The EO controller consisted of four electrode sections: the individual phase bias electrodes, the common mode azimuth beam-steering electrode, the common mode elevation beam-steering electrode and the individual amplitude control electrodes. These electrode sections are grouped in columns as is shown schematically in Figure 3.3-6.

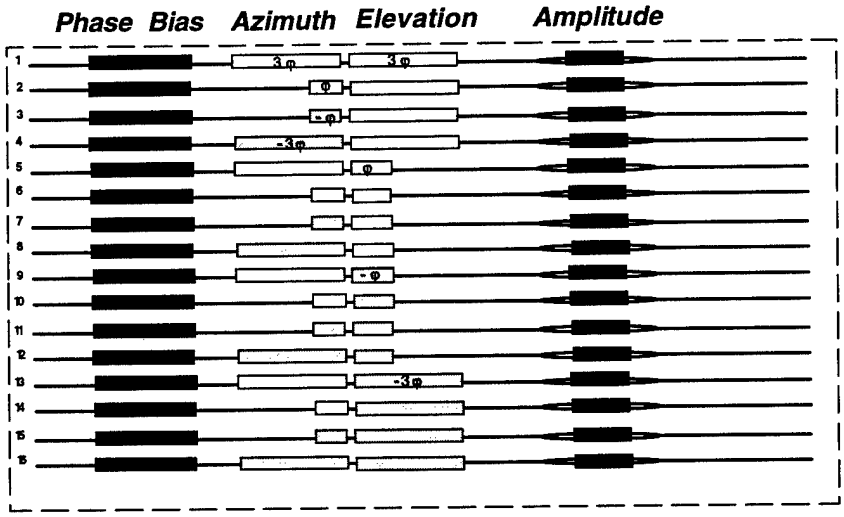

Figure 3.3-6. Electrode Sections of 16 Channel EO Controller

Measurements on the four channel IPAC in task II of this project indicated that the switching voltage V_π•length (volt-cm) product of the phase bias electrode was 12 volt-cm. The V_π is defined as the phase bias required to achieve a relative phase shift of π in the microwave signal between any two channels. The phase bias electrode in the 16 channel EO controller was designed to meet phase biasing conditions with the application of 0 to 15 volts. This makes it compatible with the many commercially available 15 volt DC sources. The two common mode electrodes (Elevation and Azimuth), as shown in Figure 3.3-6, are designed to steer the beam of a rectangular phased array with only two control signals (one for each direction). The common mode electrodes are electrically connected together. Push/pull electrodes and a linear taper approach were investigated in task II of this program. It was shown that the push/pull electrode exhibited a factor of two

improvement in efficiency as was predicted. Therefore, the push/pull design was incorporated for both beam-steering electrodes in the 16 channel IPAC.

The sixteen channel TE and TM mode polarization combiner was designed using 3M polarizing fiber packaged in a silicon v-groove by Wave Optics. The fiber axis was aligned at 45° as is shown in Figure 3.3-7.

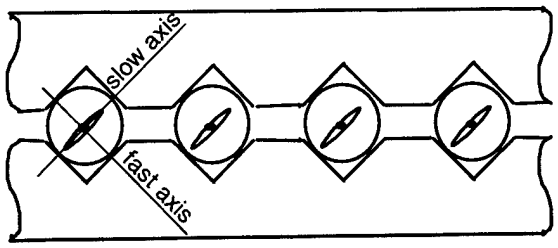

Figure 3.3-7. Endfaces of 3M Polarizing Fiber in a Silicon V-groove Array

3.4 FABRICATION AND OPTICAL TESTING OF 2-DIMENSIONAL IPAC

3.4.1 1x16 Integrated Optic Splitter

A 1x16 IOC splitter was fabricated in a z-cut LiNbO3 substrate that was optically and thermally matched to the EO controller substrate. The goal of obtaining less than 4 dB of optical insertion loss for each polarization state was achieved, and a 1x16 splitter with 1.8 dB loss for TE mode and 2.2 dB loss for TM modes was fabricated.

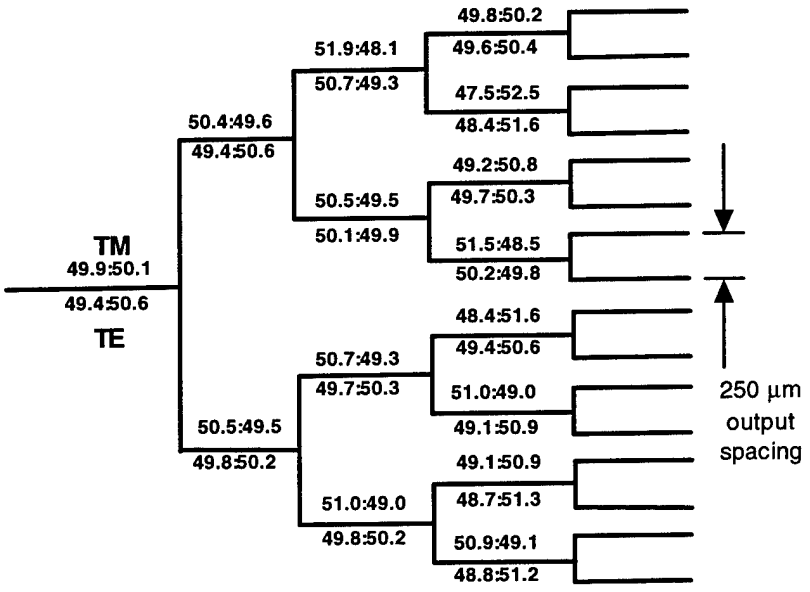

Figure 3.4.1-1. $LiNbO_3$ 1x16 Integrated Optic Splitting Ratios

Optical measurements of the splitter were taken after the polarization maintaining fiber was pigtailed to the input. In Figure 3.4.1-1, the splitting ratio for each of the Y-junctions is shown for both polarization states. All of the Y-junctions had better than a 53:47 splitting ratio.The uniformity of the splitter was measured and is shown plotted in Figure 3.4.1-2. The TE mode had a variation of less than $\pm 5.5\%$. The TM mode had a variation of $\pm 6\%$. The TM mode had slightly larger variation due to the polarization of this mode being normal to the surface of the crystal.

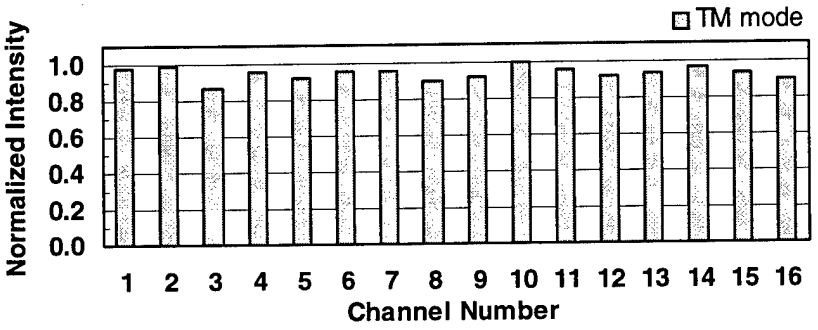

(a) TM mode uniformity

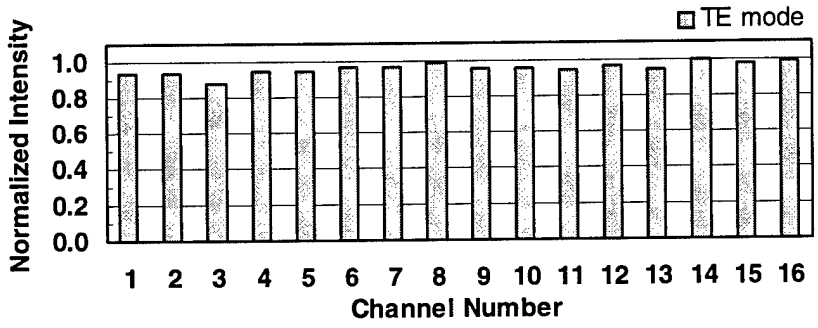

(b) TE mode uniformity

Figure 3.4.1-2. Optical Intensity Splitting Uniformity

The polarization extinction ratio was measured for each channel of the IOC splitter and found to be ≥ 30 dB after the input optical fiber was pigtailed to the splitter. The measurements are shown in Figure 3.4.1-3. Prior to pigtailing the fiber the polarization extinction ratio for the channels was found to be ≥ 35 dB. This was significantly higher than the values obtained from the SOS technology. The polarization extinction ratio of each individual channel is plotted in Figure 3.4.1-3.

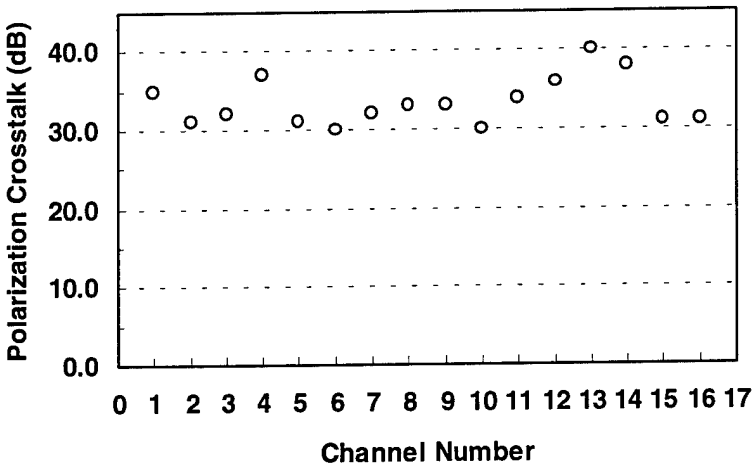

Figure 3.4.1-3. Polarization Extinction Ratio of a 1x16 $LiNbO_3$ IOC Splitter

3.4.2 Two Dimensional IPAC

The two dimensional IPAC was built using a standard 3 inch $LiNbO_3$ wafer scale fabrication process. The final IPAC is shown in Figure 3.4.2-1. The integrated optic chip is 7 cm long with four separate electrode sections.

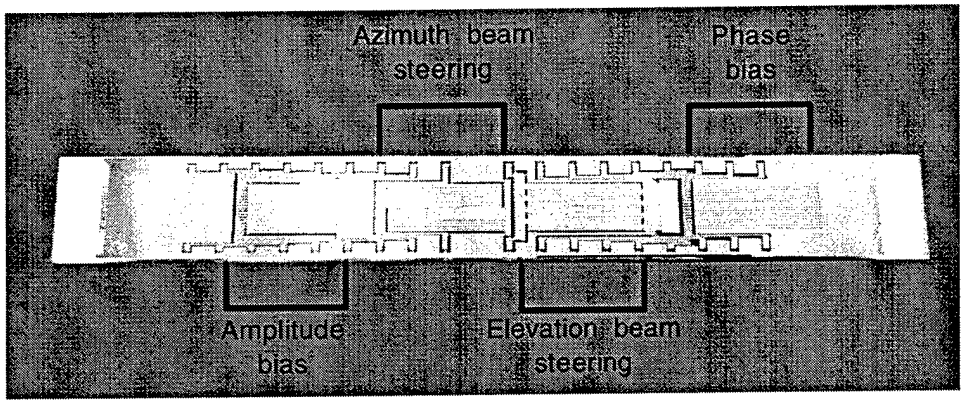

Figure 3.4.2-1. $LiNbO_3$ EO Control Submodule

The optical channels were made using a titanium indiffusion process which was optimized for the quasi-TE and quasi-TM modes based on measurements taken during task II of this program. The channels were optimized such that both polarization states were low loss, and also that the optical/electrical field overlap under the electrodes was higher for the TM modes than for the TE modes. This was done to maximize the performance of electrode sections where the desired output is related to the difference in the electro-optic phase shift between the two modes. The optical losses were measured using a single mode

polarization maintaining fiber at the input and a 100X objective lens at the output to the photodetector. The average total insertion loss per channel was 2.4 dB for the quasi-TE modes and 2.6 dB for the quasi-TM modes. The loss measurements are shown in Figure 3.4.2-2. Prior to electrical packaging of the IPAC, a $\lambda/4$ wave dielectric AR coating was applied to the endfaces of the IPAC to eliminate the Fresnel losses.

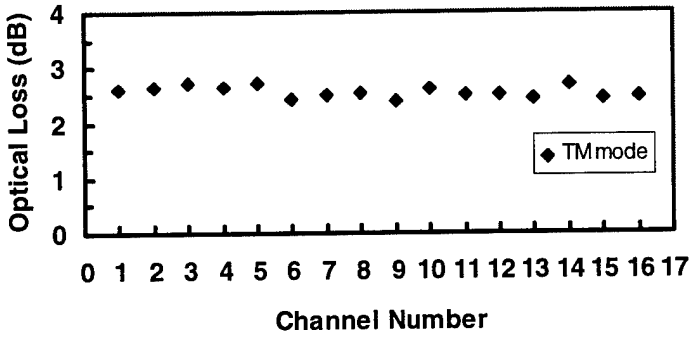

(a) TM mode optical throughput

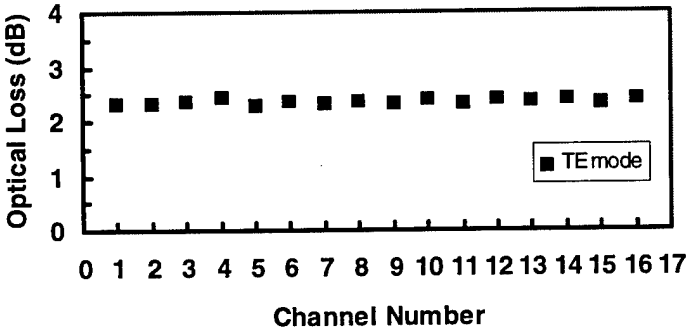

(b) TE mode optical throughput

Figure 3.4.2-2. Optical Measurements of EO Controller

An SiO_2 dielectric buffer and metallization layers were used to implement the 64 sections of electrodes on the IPAC. A schematic of these electrodes was outlined previously in Figure 3.3-6. The first section consists of 16 individual phase bias electrodes at the input. This section is used to null out the phase difference between the TE and TM mode in each channel, in addition to the phase differences from channel to channel. The V_π for the phase bias section was 12.5 volts. Following the phase bias electrodes are two common mode beam steering electrodes. One is for elevation steering, while the other is for azimuth steering. These electrodes are designed for being driven by a single voltage applied to each

one. As was shown in Figure 3.3-6, the elevation electrodes are designed to implement a linear phase taper for each group of four channels (Channels 1 to 4; 5 to 8; 9 to 12; 13 to 16). The azimuth electrode is designed to give a linear phase taper between each of the previous groups of four electrodes. In this manner these channels can be directly connected to a rectangular 4x4 phased array antenna.

At the output of the IPAC are 16 individual amplitude controllers and their mode filter sections. The amplitude controllers were implemented using Mach-Zehnder interferometers. The TM mode transfer function for channel number 1 is shown in Figure 3.4.2-3.

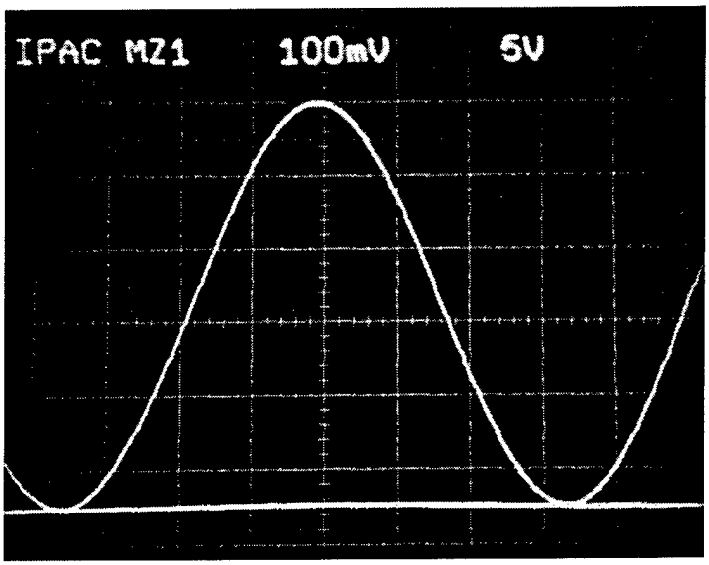

Figure 3.4.2-3. Measured TM Mode Transfer Function for Channel Number 1

The switching voltage (V_π) of the Mach-Zehnder is given by;

$$V_\pi^{TM} = \frac{\lambda G}{n_e^3 r_{33} \Gamma_{TM} L} = 17 Volts,$$

$$V_\pi^{TE} = \frac{\lambda G}{n_o^3 r_{13} \Gamma_{TE} L} > 60 Volts,$$

where λ is the optical wavelength, L is the length of the interferometer, G is the electrode gap, n is the index of refraction, r is the electro-optic coefficient and Γ is the optical/electric field overlap integral. The TM mode transfer function determines the amplitude weighting of the RF signal at the antenna element. The electrical/optical overlap function between the TE and TM modes was adjusted to insure a large phase difference between the two modes for a voltage applied to that electrode. The Mach-Zehnder sections were compacted to 4.5 mm in order to increase the length and efficiency of the other electrode sections. In general, less than 3 dB of RF amplitude adjustment is typically required at any given phased array antenna element. Therefore, much less than the V_π switching voltage is required.

3.4.3 Polarizing Fiber Array

A 16 channel polarizing fiber array was tested for uniformity and polarization extinction. The polarizing fiber was purchased from 3M. Two meter sections from the spool of optical fiber were cleaved and packaged in a fiber array with FC/PC connectors at the output. The 2-meter sections of polarizing fiber had a polarization extinction ratio of greater than 40 dB. A 1x16 splitter was butt coupled to the input of this array and the uniformity of the fiber array was measured. The de-embedded nonuniformity was found to be ± 1.1 dB for TM modes and ± 1.3 dB for TE modes. This fiber array was the least uniform component of any optical module in the phased array controller. There are two reasons for this effect. The two main sources of fiber array nonuniformity are the deviations in the fiber itself and defects in the silicon v-grooves, some examples of which are shown in Figure 3.4.3-1.

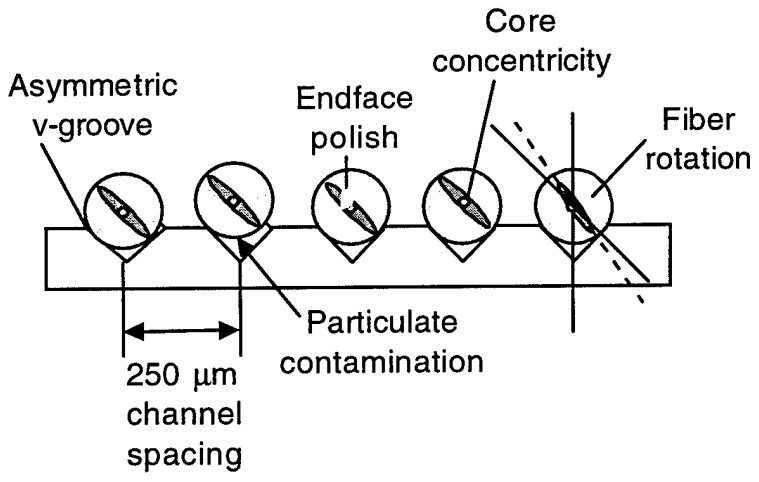

Figure 3.4.3-1. Illustration of Polarizing Fiber in Silicon V-groove Defects

There are several defects (particulate contamination, v-groove asymmetry, polish quality, rotation, etc.) in silicon v-grooves that can contribute to the translation and rotation of the

fiber in the v-groove. One alternative to using silicon v-grooves is micromachined ceramic v-grooves.

The main fiber parameter that affects the translation of the fiber in the v-groove array is the core concentricity. This specification for the experimental polarizing fiber is currently not set as tightly as that of the commercially sold PM fiber. A cross section of the polarizing fiber array is shown in Figure 3.4.3-2.

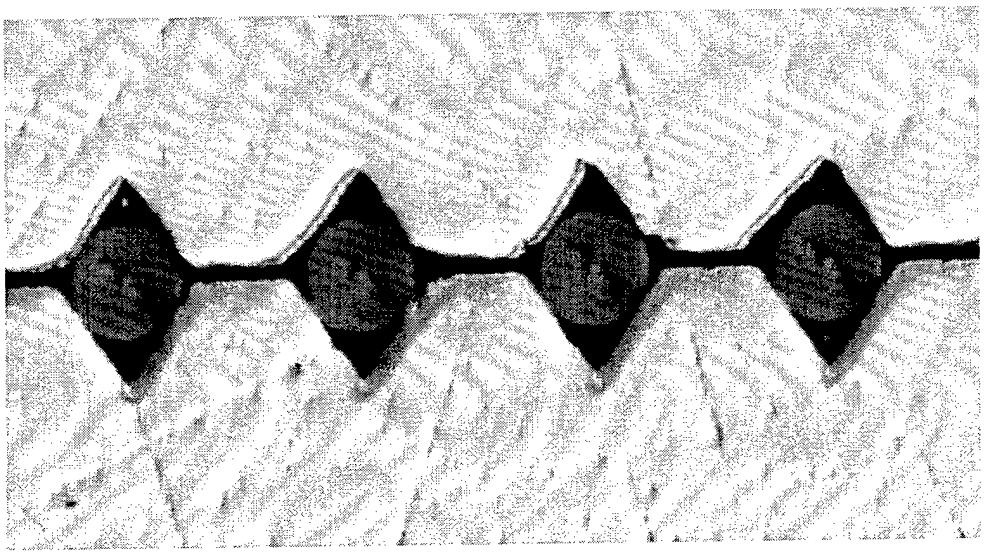

Figure 3.4.3-2. Polarizing Fiber in V-groove Array

3.5 IPAC COMMON MODULE PACKAGING

The EO controller was mounted on an aluminum subcarrier and then inserted into a gold plated Kovar package. The 38 bonding pads were bonded to the feedthroughs in the Kovar package. Double ball-stitch-ball bonds were used for each connection. The pin feedthroughs are labeled on the bottom of the package. A schematic of the labeling was provided with the delivery of the module. Upon completion of the electrical packaging, DC electrical testing was done. The phase bias electrodes were tested two at a time, using one of the channels as a reference. The RF signals were fed to the two center antenna elements of a 4 channel phased array and the signal at the receiver was nulled with the phase bias adjustment. The common mode beam steering electrodes were also DC tested in such a configuration. The amplitude controllers were tested one channel at a time. All tests were completed successfully.

The integrated optic 1x16 power splitter was fiber pigtailed with a single mode PM fiber. The 1x16 splitter was then aligned and attached onto the two dimensional EO controller. The polarization crosstalk was measured at this time and found to be $\geq$ 30 dB down for

any of the channels. A v-groove array of polarizing fiber was then pigtailed to the output of the IPAC. The total optical insertion loss was measured to be 9.3 dB for the TM modes and 8.3 dB for the TE modes. These measurements include subtracting out the 3 dB loss that is due to the 45° rotation of the output polarizing fiber. The total optical insertion loss was measured by adding the optical power together of all of the output channels relative to the net input optical power. The average optical power output of an individual channel can be calculated by dividing the total optical output power by 16 and adding 3 dB of loss associated with the 45° polarizer. The total optical loss can be subdivided into 4.2 dB (4.8 dB) loss due to the IOC chips themselves and 4.1 dB (4.5 dB) loss for the chip-to-chip coupling and polarizing fiber array attachment for TE (TM) modes respectively. The entire optical assembly was mounted on a chip carrier in the Kovar package.

Strain relief and mechanical components were added to the package prior to the sealing of the module. The final completed 16 channel IPAC Common Control Module is shown in Figure 3.5-1 both with and without the lid. This module was inserted into the phased array testbed for RF testing with various phased array antennas.

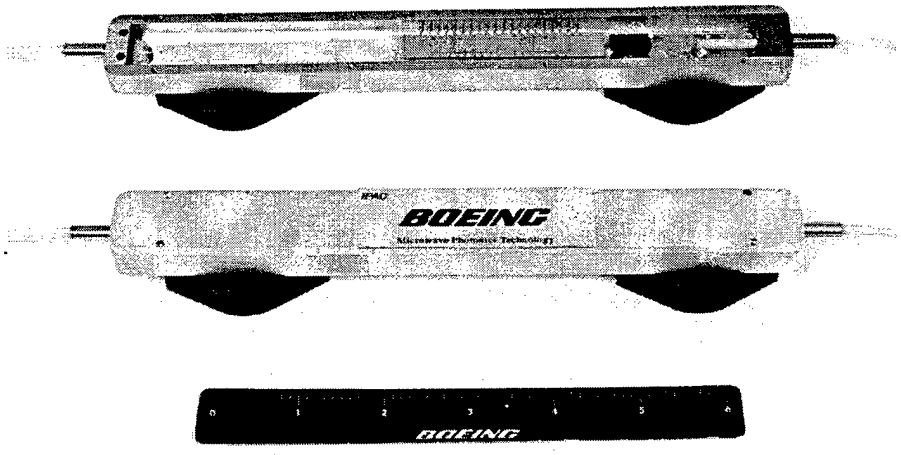

Figure 3.5-1. Packaged 16 Channel IPAC Common Control Module

4.0 PHASED ARRAY ANTENNA BEAM STEERING

4.1 U BAND PHASED ARRAY ANTENNA TESTBED

The sixteen channel IPAC architecture is designed to perform simple two dimensional beam steering of a rectangular antenna array with two control signals. A schematic of this operation is shown in Figure 4.1-1. One electrode controls the beam steering in the azimuth direction. A second electrode controls the beam steering in the elevation direction.

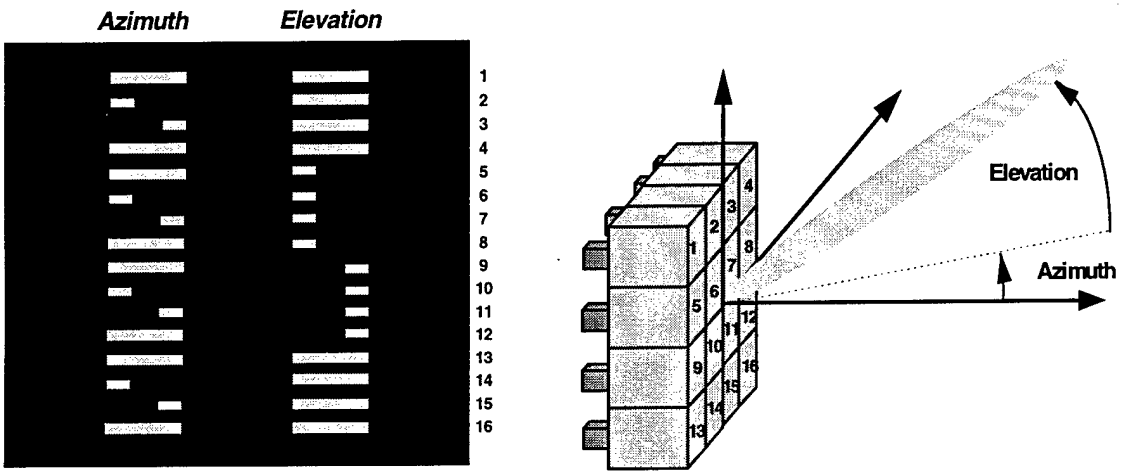

(a) Common mode electrode (b) 4x4 Phased antenna array

Figure 4.1-1. Two Dimensional Beam Steering using Common Mode Electrodes

The sixteen channels of the IPAC can be divided into groups of four. For example, channels 1 to 4; 5 to 8; 9 to 12; and 13 to 16 all share common electrodes that can be electrically connected together to perform beam steering in the vertical (elevation) direction. Similarly, channels 1-5-9-13; 2-6-10-14; 3-7-11-15; and 4-8-12-16 share common electrodes that will steer the beam in the horizontal (azimuth) direction. In this manner, two dimensional beam steering of a rectangular 16 element phased array antenna can be only two signals applied to the IPAC.

The two dimensional capabilities of the IPAC were demonstrated on a linear 4 element U band phased array antenna front end. Construction of a full 16 element rectangular phased array front end at millimeter wave frequencies for test purposes would have been prohibitively expensive for this program. The two dimensional capabilities of the IPAC can be fully demonstrated by using combinations of the four channels outlined in the previous paragraph. The front end of the U band phased array antenna, which was compatible with

the Wireless LAN frequencies of 54 to 58 GHz, is shown in Figure 4.1-2. The array consisted of a set of New Focus 60 GHz photodetectors amplified by millimeter wave amplifiers. The amplified millimeter wave signals were then fed into U band horn antennas.

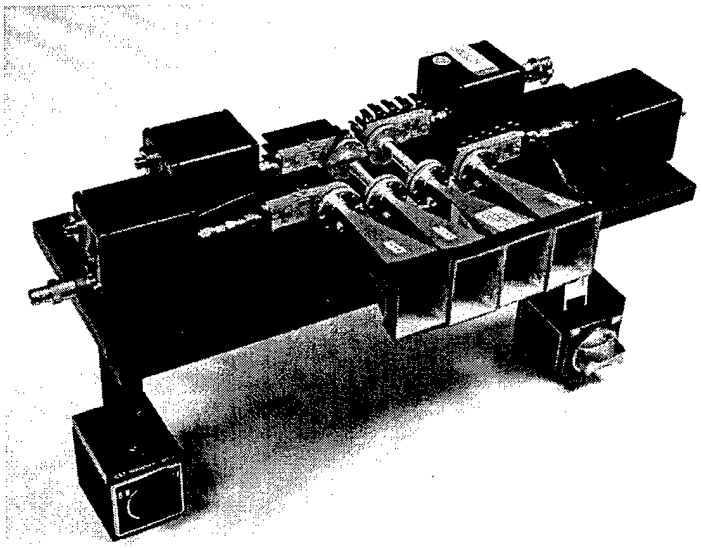

Figure 4.1-2. U Band Testbed Phased Array Antenna Front End

At the input of the testbed, two frequency offset diode pumped YAG lasers (λ=1319 nm) were used in the polarization multiplexed heterodyne system. The signals were combined and launched into the orthogonal polarization axis of a single mode polarization maintaining fiber attached to the IPAC module. The output polarizing fibers were attached four at a time to 60 GHz photodetectors of the phased array antenna front end. The receiver consisted of a horn antenna with its output fed into a downconverter for conversion of the received signal into an IF signal. The IF signal is fed into a spectrum analyzer and stored on a personal computer. In a similar manner that was demonstrated in task II of this program, an application of a single sawtooth signal to the IPAC will sweep the antenna pattern across the receiver. This antenna pattern is then stored onto a computer.

4.2 TWO DIMENSIONAL ANTENNA BEAM STEERING DEMONSTRATION

The main lobe of the four element antenna can be steered with one signal applied to either the elevation or azimuth beam control electrode, depending on which channels are chosen. A DC voltage applied to one of these electrodes will determine the pointing direction of the main lobe proportional to the magnitude of the voltage. The two dimensional beam steering capability of the IPAC module is demonstrated by connecting the appropriate channels of the IPAC into the four photodetectors of the 4 element linear phased array. In demonstrating azimuth beam steering the channels were grouped from 1 to 4; 5 to 8; 9 to 12; and 13 to 16. The same azimuth electrode was addressed in each case. The four

resulting antenna patterns are as shown in Figure 4.2-1. In a rectangular 16 element antenna array, all four rows of the array would be steered in the azimuth direction with a single signal applied to the azimuth electrode. The center frequency for all of the antenna pattern measurements shown in Figures 4.2-1 and 4.2-2 was 50 GHz.

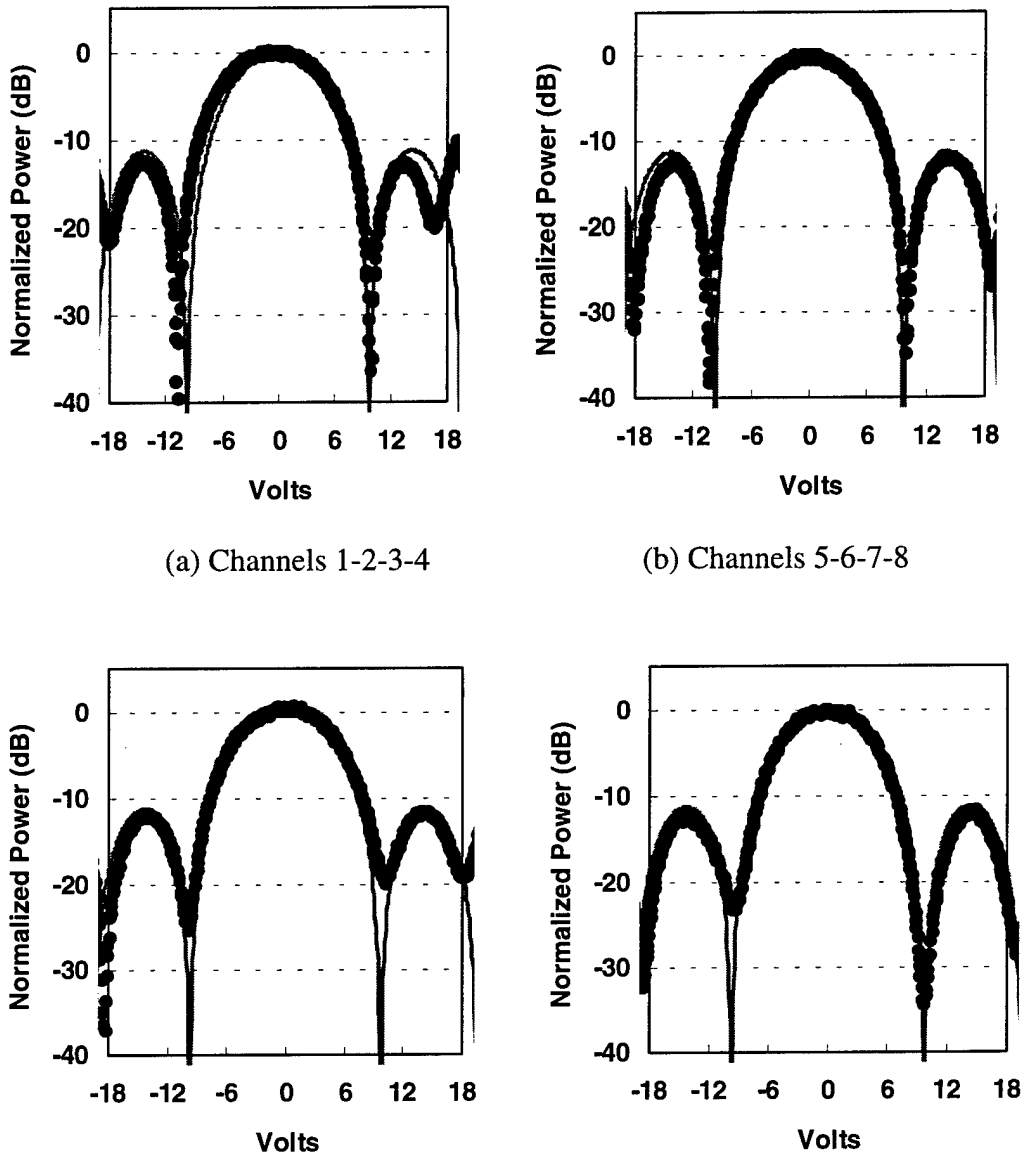

(a) Channels 1-2-3-4

(b) Channels 5-6-7-8

(c) Channels 9-10-11-12

(d) Channels 13-14-15-16

Figure 4.2-1. Two Dimensional Azimuth Beam Steering

The beam steering capability of the 16 channel IPAC was demonstrated for the elevation direction in a similar manner. The channels were fed into the photodetectors four at a time; 1-5-9-13; 2-6-10-14, 3-7-11-15; and 4-8-12-16. These corresponded to the columns

of a two dimensional 4x4 rectangular phased array. The antenna beam pattern measurements are shown in Figure 4.2-2. Similar to the azimuth direction the application of a common signal to the elevation electrode will steer all of the columns of a 16 element antenna array in the elevation direction. The solid line in the plots is the calculated antenna pattern which shows a good fit to the measured data.

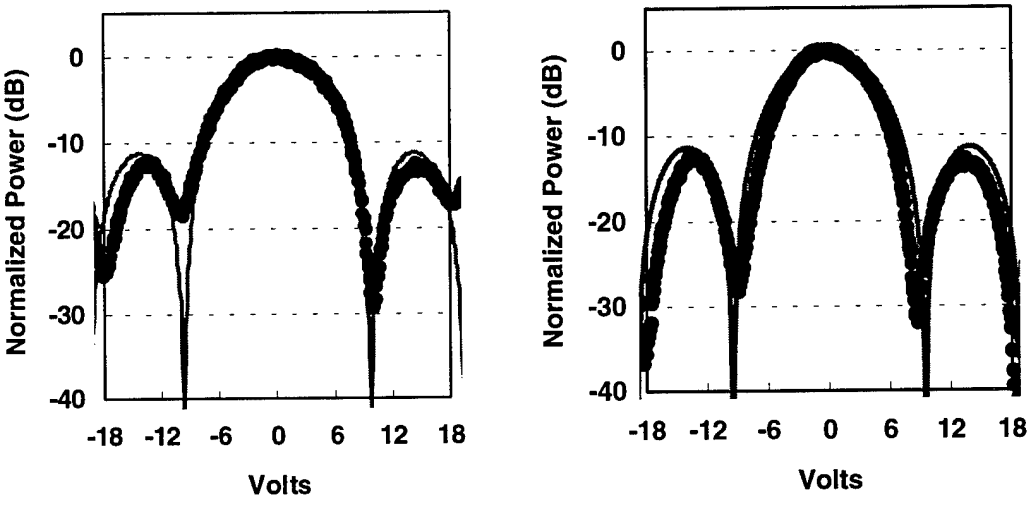

(a) Channels 1-5-9-13

(b) Channels 2-6-10-14

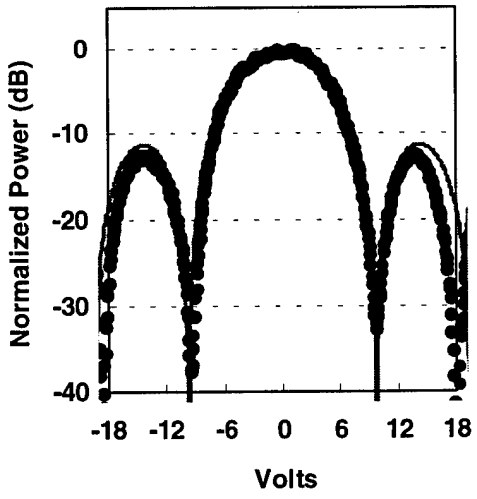

(c) Channels 3-7-11-15

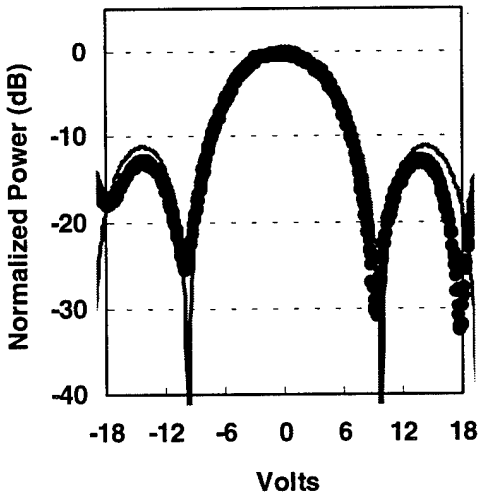

(d) Channels 4-8-12-16

Figure 4.2-2. Two Dimensional Elevation Beam Steering

4.3 OPTICAL CONTROL FOR ANTENNA SIDELOBE SUPPRESSION

The sidelobe level of the antenna beam pattern can be controlled by applying an amplitude taper across the array. The amount of sidelobe level suppression and center lobe shape will be determined by the mathematical form of the taper. The IPAC module contains a photonic amplitude controller for these operations. Each channel of the IPAC module has its own separate amplitude controller. The four element testbed array was used in a simple demonstration of these functions. Four channels of the IPAC were sent to the phased array antenna elements. The photonic amplitude controllers were originally set such that the microwave signals of the two center elements and two outer elements were equal. Then the microwave amplitude of the two outer antenna elements was switched to 70% of the value of the two interior antenna elements using the photonic controllers on the IPAC. A switching time of less than 1 microsecond can be used. The switching speed is only limited by the bandwidth of the Mach-Zehnder photonic amplitude controller. An antenna pattern with suppressed sidelobe levels was measured and is shown below in Figure 4.3-1.

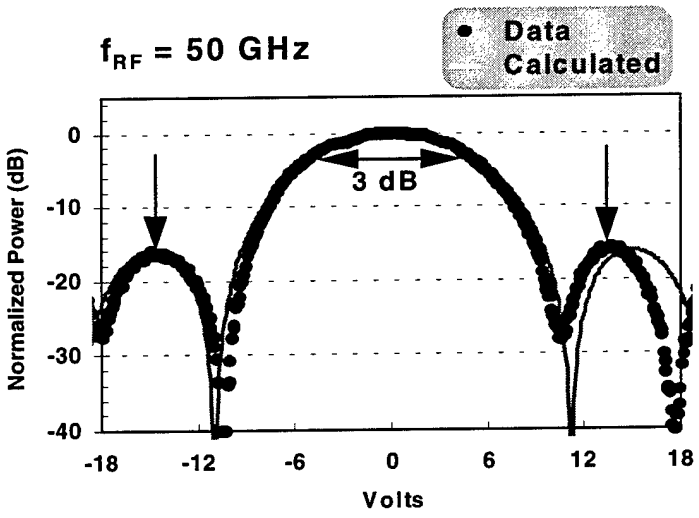

Figure 4.3-1. Photonically Controlled Amplitude Taper for Antenna Sidelobe Reduction

As shown in Figure 4.3-1, the main antenna lobe was spread out and the primary sidelobe levels were reduced by several dB relative to the main lobe. The measured data is a good fit to the calculated values. Additional amplitude tapers such as binomial and Dolph-Chebyshev amplitude tapers can easily be implemented. It should also be noted that much greater sidelobe suppression is obtainable with antenna arrays containing a greater number of elements.

4.4 IPAC DEMONSTRATION FOR RAP RADIO (6 to 12 GHz)

One very important feature of the IPAC is that it is a Common Module. The same physical IPAC can be used over a very wide (RF, microwave, and millimeter wave) frequency range. This should offer cost savings since the same IPAC would be fabricated regardless of the center frequency of the phased array antenna. The center frequency is set by the offset of the diode pumped Nd:YAG solid state lasers. A demonstration of this concept was achieved by using the same IPAC that was used in the Wireless LAN (54 to 58 GHz) demo, to steer a phased array antenna that was operational at RAP Radio frequencies (6 to 12 GHz). The phased array antenna testbed that was used in the Wireless LAN demo was modified for use at 7 GHz. A photograph of this setup is shown in Figure 4.4-1.

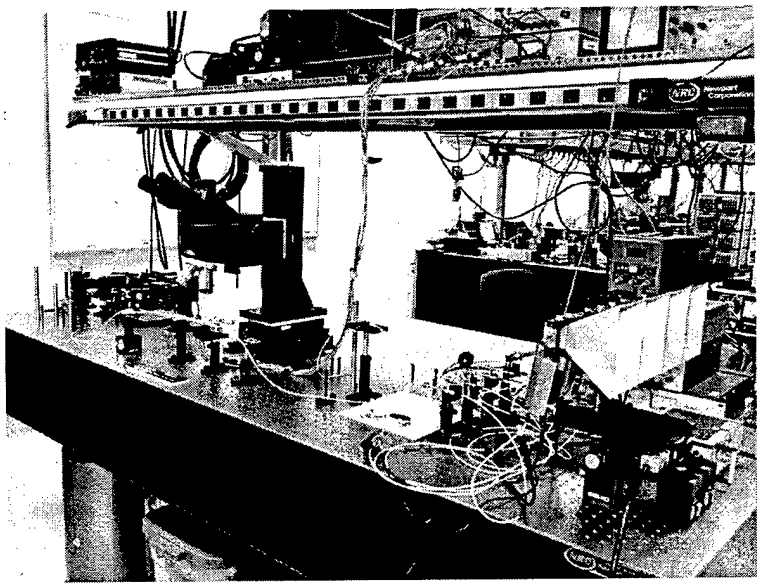

Figure 4.4-1. Phased Array Antenna Testbed for RAP Radio Frequencies (6 to 12 GHz)

The changes to the front end of the phased array antenna consisted of using BT&D 12 GHz photodetectors, off-the-shelf Avantek amplifiers, and C band horn antennas. The receiver was a C band horn antenna with no further downconversion. The remainder of the setup (IPAC and lasers) remained the same. Using the same technique that was reported previously, a signal could be applied to the IPAC and the antenna beam could be swept across the receiver. The resulting antenna pattern at 7 GHz and a schematic of the measurement technique are shown in Figure 4.4-2.

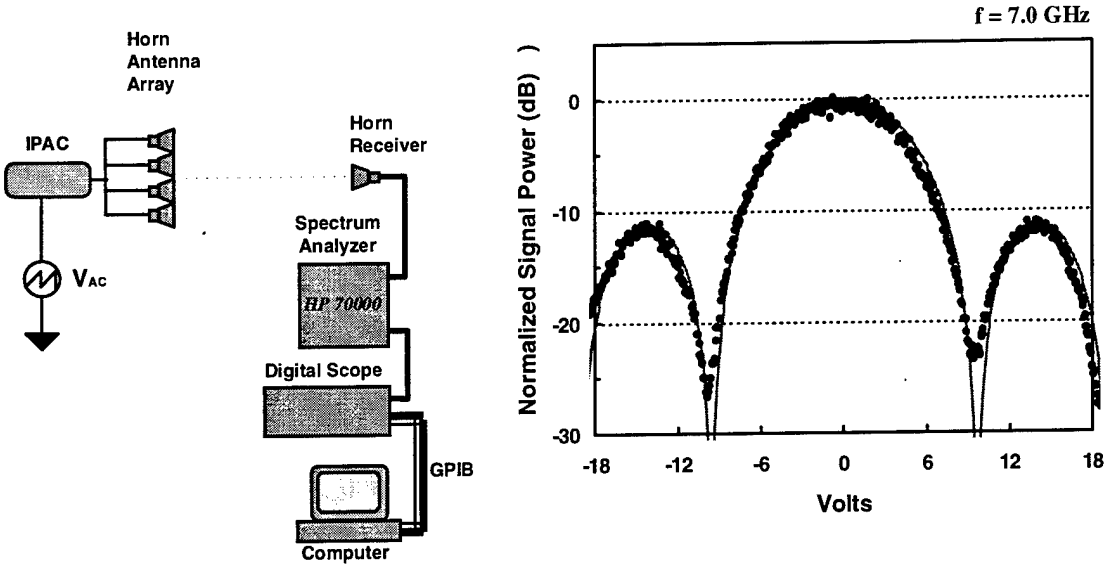

Figure 4.4-2. Swept Antenna Pattern with Measurement Setup at RAP Radio Frequencies

In a more typical test setup used in antenna ranges, the phased array antenna beam is pointed in a particular direction, and the transmitting antenna is rotated to measure the resulting antenna pattern. Such a set was constructed in order to measure the beam pointing capabilities of the IPAC Control Module. A diagram of this setup in addition to a measured antenna pattern for the 4 element C band horn antenna array with no signal applied to the IPAC is given in Figure 4.4-3. The horn array front end was mounted on an automated rotation stage. The RF signal from the receive horn was fed into an RF power meter. This signal was read out by a computer in synchronization to the rotation of the phased array antenna front end.

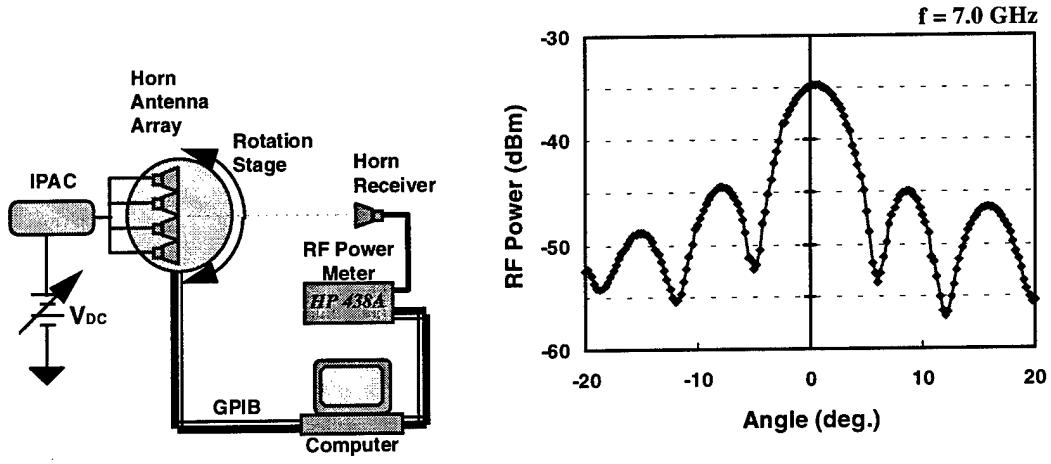

Figure 4.4-3. Antenna Array Pattern Measurement System and Four Element Horn Antenna Array Pattern

A single DC voltage was applied to the IPAC resulting in the pointing of the antenna array main lobe in a corresponding direction. In Figure 4.4-4, the phased array antenna pattern is scanned both before and after the application of 15 volts to the IPAC electrode. The center lobe of the four element antenna array is shifted from broadside to pointing at 12° relative to the centerline of the axis. The grating lobes also come up due to the number of elements and spacing of the four element array.

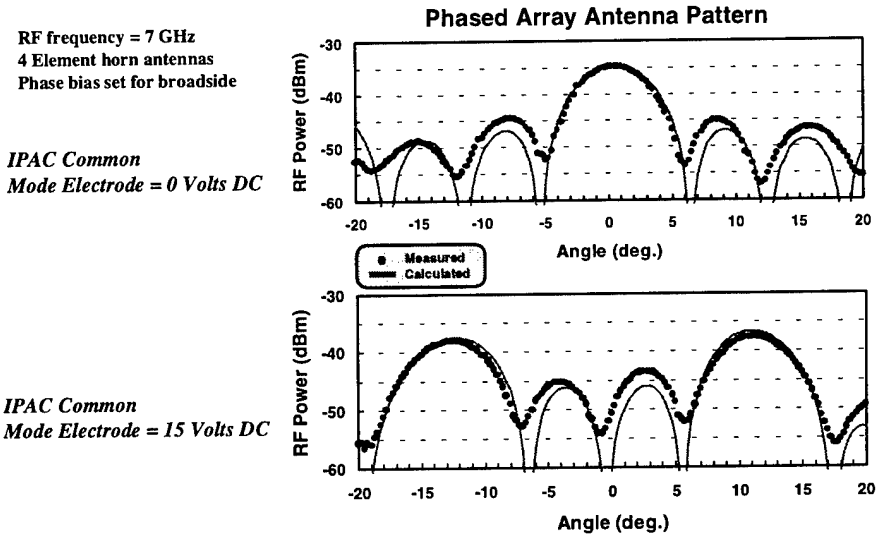

Figure 4.4-4. Antenna Beam Pointing as a Function of Applied DC Voltage

The pointing angle of the antenna beam versus the voltage applied to the IPAC is determined by the geometry of the phased array. In our test setup, the spacing between the horn antennas was 2.5λ at 7 GHz. A plot of the array factor for four antenna elements is given in Figure 4.4-5a. In the figure, the grating lobes occur at 22° because of the element spacing. Therefore, for this antenna spacing the optical channels are phase shifted by 180° when 15 volts is applied to the IPAC the main lobe is pointed by 12°. A phased array with a λ/2 spacing between elements would have an array factor such as the one shown in Figure 4.4-5b. In this array, the application of ±12 volts to the IPAC would point the beam by ±90°. In general, it is desirable to maintain an antenna element spacing of one half wavelength or less to eliminate the grating lobes in the visible region.

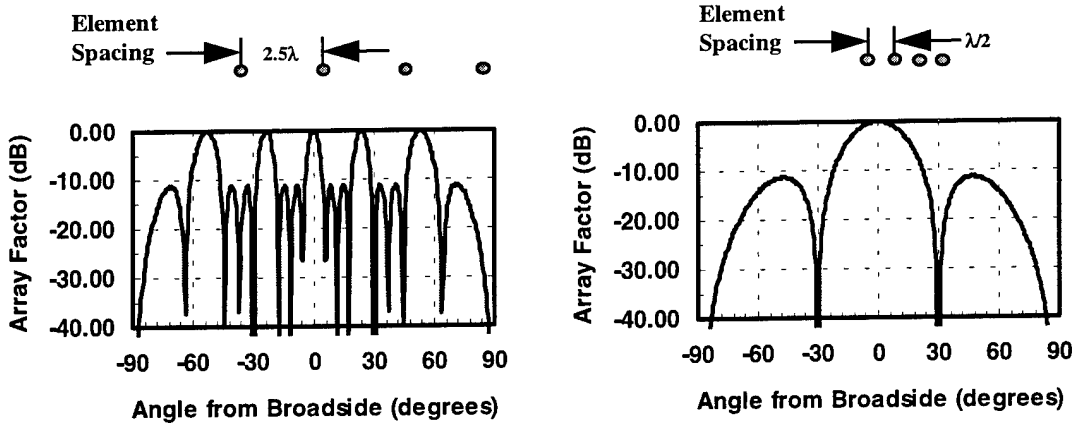

(a) Array Factor for 2.5λ Element Spacing (b) Array Factor for λ/2 Element Spacing

Figure 4.4-5. Four Element Phased Antenna Array Factor for 2.5λ and λ/2 Spacing Between Antenna Elements

The antenna main lobe pointing angle as a function of applied DC voltage is shown in Figure 4.4-6. The pointing angle is a linear function of the applied DC voltage. Therefore, one can synthesize many different waveforms to drive the IPAC with and point the main lobe of a phased array antenna in many different directions at a very high rate.

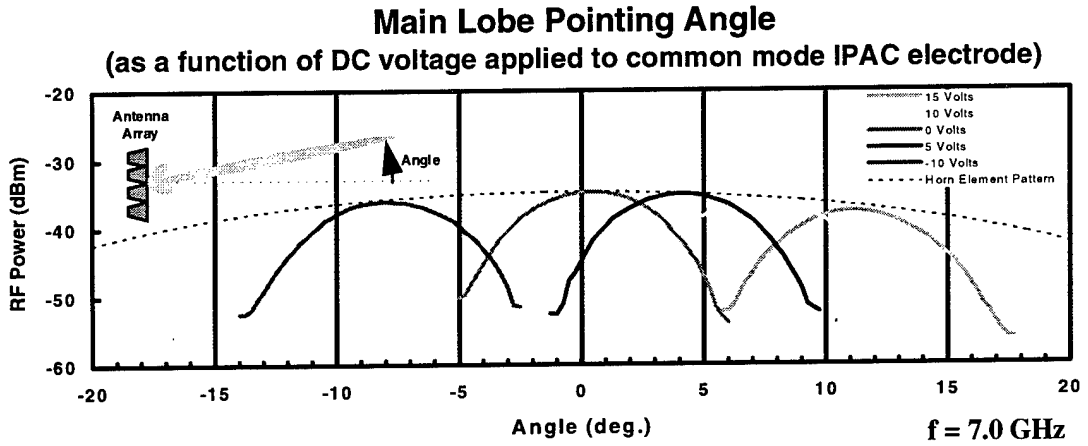

Figure 4.4-6. Main Lobe Pointing Angle versus Various Applied Voltages to the IPAC

5.0 CONCLUSIONS

A photonic module for performing beam forming and steering operations in phased array antenna systems offers advantages such as:

- elimination of dispersive electronic phase shifters and amplitude controllers,
- a reduced volume requirement for each antenna element,
- the ability to remote beam steering operations away from antenna front end,
- the use of fiber optic corporate feed networks,
- new simplified signal processing schemes, and
- a common module for operation that is independent of the center frequency.

In this program we have developed and demonstrated such a module. A 16 channel two dimensional IPAC common control module was developed for controlling a two dimensional phased array antenna. The beam steering operations of the module were demonstrated at both 7 GHz and 40 to 60 GHz corresponding to frequencies used for RAP Radio and Wireless LAN.

Two dimensional operation of the photonic IPAC was demonstrated by coupling the appropriate channels into a 4 element linear phased array. RF phase shifting and amplitude control were both demonstrated with the photonic IPAC module. The amplitude controllers were used to reduce the side lobe level of a phased array system consisting of horn antennas. Antenna array beam steering operations were demonstrated using a novel technique employing a single signal applied to a common mode electrode. This technique is a precursor to many other operations that can be performed during phased array antenna beam steering. A simple demonstration of this was the application of a DC voltage to the IPAC corresponding to a main antenna lobe pointing angle. The only limitation to the speed of these operations is the bandwidth (>100 MHz) of the electro-optic devices used in the photonic IPAC.

Finally, it should be noted that the IPAC module has the advantage that it can be scaled to operate on much larger phased array antenna systems, without a significant change in the size of this common control module.

6.0 REFERENCES

1. 1991 U.S. Patent Application, Boeing Invention Disclosure No. D91-199, "Phased Array Beam Controller Using Integrated Electro-Optic Circuits," by Suwat Thaniyavarn.

2. S. Thaniyavarn, G. Abbas, and B. Dougherty, "Electro-optic Control of Microwave and Millimeter-wave Signals using Integrated Optical Waveguide Components," *SPIE 1291-17 - Optical & Digital GaAs Technologies for Signal-Processing Applications*, Orlando, April 1990.

3. T.J. Tayag, D.M. Mackie, and G.W. Bryant, "A Manufacturable Technique for Implementing Low-Loss Self-Imaging Waveguide Beamsplitters," *IEEE Photonics Technology Letters*, vol. 7, no. 8, August 1995.